DOI: 10.1002/((please add manuscript number))

Article type: Communication

Ternary System with Controlled Structure: A New Strategy towards Efficient Organic Photovoltaics

*Pei Cheng, Rui Wang, Jingshuai Zhu, Wenchao Huang, Sheng-Yung Chang, Lei Meng, Pengyu Sun, Hao-Wen Cheng, Meng Qin, Chenhui Zhu, Xiaowei Zhan and Yang Yang**

[*] Dr. P. Cheng, R. Wang, Dr. W. Huang, S. Chang, Dr. L. Meng, P. Sun, H. Cheng, Dr. M. Qin, Prof. Y. Yang

Department of Materials Science and Engineering

University of California

Los Angeles, CA 90095, USA

E-mail: yangy@ucla.edu

Dr. W. Huang, H. Cheng, Prof. Y. Yang

California NanoSystems Institute

University of California

Los Angeles, CA 90095, USA

J. Zhu, Prof. X. Zhan

Department of Materials Science and Engineering

College of Engineering

Key Laboratory of Polymer Chemistry and Physics of Ministry of Education

Peking University

Beijing, 100871, P. R. China

Dr. C. Zhu

Advanced Light Source

Lawrence Berkeley National Laboratory

Berkeley, CA 94720, USA

Pei Cheng and Rui Wang contributed equally to this work

Recently, a new type of active layer with a ternary system has been developed to further enhance the performance of binary system organic photovoltaics (OPV). In the ternary OPV, almost all active layers are formed by simple ternary blend in solution, which eventually leads to the disordered bulk heterojunction (BHJ) structure after a spin-coating process. There are two main restrictions in this disordered BHJ structure to obtain further higher performance OPV. One is the isolated second donor or acceptor domains. The other is the invalid metal-semiconductor contact. Herein, the concept and design of donor/acceptor/acceptor ternary OPV with more controlled structure (C-Ternary) is reported. The C-Ternary OPV is fabricated by a sequential solution process, in which the second acceptor and donor/acceptor binary blend are sequentially spin coated. After the device optimization, the power conversion efficiencies (PCEs) of all OPV with C-Ternary are

enhanced by 14–21% relative to those with the simple ternary blend; the best PCEs are 10.7% and 11.0% for fullerene-based and fullerene-free solar cells, respectively. Moreover, the averaged PCE value of 10.4% for fullerene-free solar cell measured in this study is in great agreement with the certified one of 10.32% obtained from Newport Corporation.

Keywords: organic solar cells; organic photovoltaics; non-fullerene; ternary; sequentially process

Photovoltaic (PV) energy is one of the promising renewable energy sources, among the thin film photovoltaics, the solution-based organic photovoltaics (OPV) have attracted considerable attentions due to some potential advantages, such as low-cost and light-weight, flexible and possible semi-transparent, fast and large-area fabrication.[1-8] To date, OPV have shown the best performance with certified power conversion efficiency (PCE) of around 11.5%.[9]

The history of OPV can be divided into three stages by the compositions of the active layer. At the early stage of OPV research (1950s–1980s), the active layer consisted of only a single organic semiconductor (p-type or n-type). Such OPV yielded a very low PCE due to the insufficient exciton dissociation by the electrical field, which was caused by the large binding energy of organic semiconductor.[10] In 1980s[11] and 1990s,[12, 13] the active layer with donor/acceptor binary system was employed in the OPV. Because of the increased donor/acceptor interfaces in the active layer, the exciton dissociation in binary system solar cells became much more efficient than that in the single organic component solar cells. In

recent years, a new type of active layer with ternary system was developed to further enhance the performance of binary system OPV.[14-18] Compared to the binary system solar cells, the solar cells with ternary system present several advantages including the broader and stronger optical absorption, efficient charge separation, transportation and extraction, and improved device stability.[16] The ternary OPV can be classified by the type of the third component: donors,[19-25] acceptors,[26-29] inorganic materials[30-32] and nonvolatile additives.[33-38] Among them, the most representative third component is the second donor or acceptor.

In the ternary OPV, almost all active layers are formed by simple ternary blend in the solution, which eventually leads to the disordered bulk heterojunction (BHJ) structure after a spin-coating process (see **Figure 1a**). Although this disordered BHJ structure has widely existed in high performance ternary OPV, there are still two main restrictions for a further higher performance.[39-41] One is the isolated second donor or acceptor domains (shown as green parts in Figure 1a), which acts as traps for the charge recombination and hardly contribute to the photocurrent in solar cells. The other is the invalid metal-semiconductor contact (second donor at cathode or second acceptor at anode), which is bad for efficient charge extraction. Thus, in order to further enhance the device efficiency, ternary OPV with more controlled structure is highly desired.

Herein, we report the concept and design of donor/acceptor/acceptor ternary OPV with a more controlled structure (C-Ternary OPV). The C-Ternary OPV (**Figure 1b**) is fabricated by sequential solution process,[42-48] in which the third component (second acceptor) and donor/acceptor binary blend are sequentially spin coated by orthogonal solvents. In order to demonstrate the generality of the C-Ternary, four different donor/acceptor/acceptor blends

are employed in OPV. After device optimization, the PCEs of all four OPV with C-Ternary are enhanced by 14–21% relative to those with simple ternary blend (S-Ternary); the best PCEs are 10.7% and 11.0% for fullerene-based and fullerene-free solar cells, respectively. Moreover, the averaged PCE value of 10.4% for fullerene-free solar cell measured in this study is in great agreement with the certified one of 10.32% obtained from Newport Corporation (see Supplementary Information). Our work demonstrates that the C-Ternary is a potential alternative to the simple ternary blend used in OPV with much higher efficiency.

Figure 1

The chemical structures of materials used in this work are shown in **Figure 1c**. The energy levels of materials used in this work are shown in **Figure S1** (Supporting Information). Polymer PTB7-Th[49] or PBDB-T[50] is used as the donor; small molecule ITIC[51] or $PC_{71}BM$ is used as the acceptor; small molecule IDIC[52] is used as the third component (second acceptor). Since IDIC is slightly soluble in o-dichlorobenzene (DCB) (which can be proved by UV absorbance tests before and after the spin-coating of neat DCB, **Figure S2**, Supporting Information), the donor/acceptor binary blend can be spin coated on IDIC layer to form the C-Ternary OPV with DCB as the processing solvent. **Figure 2** shows the *J–V* curves and the external quantum efficiency (EQE) spectra of devices based on PTB7-Th: $PC_{71}BM$ (binary blend (Binary)), PTB7-Th: $PC_{71}BM$: IDIC (S-Ternary) and PTB7-Th: $PC_{71}BM$/IDIC (C-Ternary) under the illumination of an AM 1.5G solar simulator, 100 mW cm^{-2}. The average and the best device characteristics of PTB7-Th: $PC_{71}BM$ or PTB7-Th: ITIC without or with IDIC as the third component (S-Ternary or C-Ternary) are summarized in **Table 1**. The average and the best device characteristics of PBDB-T: $PC_{71}BM$ or PBDB-T: ITIC without or

with IDIC as the third component (S-Ternary or C-Ternary) are summarized in **Table 2**. The average device data are calculated from 15 individual devices. For PTB7-Th based OPV (PTB7-Th/$PC_{71}BM$ and PTB7-Th/ITIC), the S-Ternary devices exhibit slightly higher average PCE (9.0% and 7.8%) than that of the Binary devices (8.8% and 7.6%), resulted from the increased short circuit current density (J_{SC}) but decreased fill factor (FF). After the device optimization (Table S1, Supporting Information), the C-Ternary devices exhibit boosted performance compared with S-Ternary devices. The average J_{SC} increases from 17.5 to 18.7 mA/cm^2 and 16.3 to 17.6 mA/cm^2 for $PC_{71}BM$ and ITIC based devices, respectively. The average FF increases from 64.9% to 69.6% and 60.0% to 64.2% for $PC_{71}BM$ and ITIC based devices, respectively. As a result, the C-Ternary devices exhibit much higher average PCE (10.3% and 9.0%) than that of the S-Ternary devices (9.0% and 7.8%). The best PCEs of the C-Ternary devices are as high as 10.7% and 9.5% for $PC_{71}BM$ and ITIC based devices, respectively. For the PBDB-T based OPV (PBDB-T/$PC_{71}BM$ and PBDB-T/ITIC), the trend is similar. S-Ternary devices exhibit slightly higher average PCE (7.0% and 8.9%) than that of the Binary devices (6.7% and 8.8%); C-Ternary devices exhibit much higher average PCE (8.5% and 10.4%) than that of the S-Ternary devices (7.0% and 8.9%). The best PCEs of the C-Ternary devices are as high as 9.0% and 11.0% for $PC_{71}BM$ and ITIC based devices, respectively. In addition, the C-Ternary PBDB-T: ITIC/IDIC device without the encapsulation was sent to the Newport Corporation for certification. A certified PCE of 10.32 ± 0.27% was obtained with a J_{SC} of 15.75 ± 0.33 mA cm^{-2}, V_{OC} of 0.9071 ± 0.0062 V, and FF of 72.3 ± 0.4% (**Figure S3**, Supporting Information). The certified PCE value is similar to the average value (10.4%) obtained from our laboratory. As shown in **Figure 2b**, the trend

observed in EQE is similar to the one in the J_{SC}. In the range of 450 to 750 nm, the observance of strong EQE is mainly due to the PTB7-Th and IDIC, while EQE below the 450 nm stems from the $PC_{71}BM$. The EQE is enhanced by the incorporation of the third component IDIC. The calculated J_{SC} values obtained from the integration of the EQE spectra with the AM 1.5G reference spectrum are close to the measured values (the average mismatch is 2.3%, Table 1 and 2). In addition, the EQE spectrum of a binary blend device based on PTB7-Th/IDIC is shown in **Figure S4** (Supporting Information).

Figure 2

Table 1

Table 2

Figure 3a shows the ultraviolet–visible (UV–vis) absorption spectra of pure PTB7-Th, $PC_{71}BM$ and IDIC films. $PC_{71}BM$ shows visible absorption, while PTB7-Th and IDIC show visible as well as near infrared absorption. Compared with the PTB7-Th, IDIC exhibits slightly red-shifted absorption (by 10 nm). The absorption spectra of PTB7-Th: $PC_{71}BM$ (Binary, 100 nm), PTB7-Th: $PC_{71}BM$: IDIC (S-Ternary, 115 nm) and PTB7-Th: $PC_{71}BM$/IDIC (C-Ternary, 115 nm) films are shown in **Figure 3b**. The thicknesses of these blended films are the same as the ones used in their corresponding best devices. Compared with the Binary film, the S-Ternary and C-Ternary films exhibit stronger absorptions in 600-750 nm regions, which contribute to the higher J_{SC} and EQE. Photoluminescence (PL) quenching efficiency was employed to investigate the charge separation proportions in different films. As shown in **Figure 3c**, the PL intensities of PTB7-Th: $PC_{71}BM$ (Binary), PTB7-Th: $PC_{71}BM$: IDIC (S-Ternary) and PTB7-Th: $PC_{71}BM$/IDIC (C-Ternary) films

decrease by 94%, 78% and 94%, respectively, relative to that of the pure PTB7-Th film. The strong PL quenching (94%) of Binary and C-Ternary films suggests the efficient charge separation, while the PL quenching of S-Ternary film is insufficient (78%), which may be resulted from the invalid charge separation at the interface of donor and isolated third component (the second acceptor) domains.

Figure 3

Space charge limited current (SCLC) method[53] was employed to measure the hole and electron mobility of PTB7-Th: $PC_{71}BM$ (Binary), PTB7-Th: $PC_{71}BM$: IDIC (S-Ternary) and PTB7-Th: $PC_{71}BM$/IDIC (C-Ternary) films. Hole-only and electron-only diodes were fabricated using the architectures of indium tin oxide (ITO)/poly(3,4-ethylenedioxythiophene): poly(styrene sulfonate) (PEDOT: PSS)/active layer/gold (Au) for holes and aluminum (Al)/active layer/Al for electrons. The dark *J–V* curves of the devices are plotted as $\ln[Jd^3/(V_{appl}-V_{bi})^2]$ versus $[(V_{appl}-V_{bi})/d]^{0.5}$ (**Figure 4a** and **4b**). The hole mobilities and electron mobilities are calculated and listed in **Table 3**. The hole mobility and electron mobility of the Binary and C-Ternary films are similar (4.1×10^{-3} *vs.* 3.7×10^{-3} $cm^2V^{-1}s^{-1}$ for hole; 5.5×10^{-4} *vs.* 4.1×10^{-4} $cm^2V^{-1}s^{-1}$ for electron), while the S-Ternary film exhibits much lower hole mobility (2.0×10^{-4} $cm^2V^{-1}s^{-1}$) and lower electron mobility (7.5×10^{-5} $cm^2V^{-1}s^{-1}$) compared to that of the C-Ternary film. There are two main factors affecting the charge transportation: molecular packing and transportation pathways. The molecular packing of films is characterized using the grazing-incidence wide-angle X-ray scattering (GIWAXS) patterns. As shown in **Figure 4c**, the molecular packing behavior in Binary, S-Ternary and C-Ternary films is similar in terms of the polymer crystallite orientation and the $PC_{71}BM$

aggregation. It is indicated by the similar ring-like lamellar peak at q = 0.3 $Å^{-1}$ and characteristic PCBM diffraction ring at q = 1.3 $Å^{-1}$. Because of the similarity in molecular packing behavior, the much lower mobility (especially the hole mobility) of the S-Ternary film is hypothesized to be caused by the presence of the isolated third component (the second acceptor) domains. These act as traps for charge recombination and restrict the charge transportation pathways. Attributed to higher hole and electron mobility of C-Ternary device compared with that of S-Ternary device, higher FF (ca. 70%) can be achieved.

Figure 4

Table 3

In order to compare the vertical distribution[54-58] of the Binary, S-Ternary and C-Ternary films, X-ray photoelectron spectroscopy (XPS) was used to measure the ratio of atoms at the bottom surface of the active layers (**Figure 5**). The lift-off process in water was used to prepare the samples for XPS tests. Since PTB7-Th, $PC_{71}BM$ and IDIC all contain oxygen (O), while only PTB7-Th contains fluorine (F), and only IDIC contains nitrogen (N), we attribute the O1s spectral line (≈530 eV) to PTB7-Th, $PC_{71}BM$ and IDIC, F1s spectral line (≈690 eV) to PTB7-Th, and N1s spectral line (≈400 eV) to IDIC. One PTB7-Th repeated unit contains one F atom and two O atoms; one $PC_{71}BM$ molecule contains two O atoms; and one IDIC molecule contains four N atoms and two O atoms. We calculated the donor polymer PTB7-Th molar content at the bottom surface from the O/F ratio (details in the Supporting Information). The result indicates that there is a large proportion of the donor polymer (48.3% and 46.1%) in the bottom surface of Binary and S-Ternary films, which is unfavorable for charge extraction at cathode. Thanks to the structure of the C-Ternary film,

the vertical distribution of active layer becomes much better (no donor polymer locates at the bottom surface). This is beneficial for the efficient charge extraction at cathode, resulting in much higher J_{SC}, FF and PCE compared to that of the Binary or S-Ternary based device.

Figure 5

To further investigate the charge separation and collection (transportation and extraction) efficiencies in Binary, S-Ternary and C-Ternary devices, corrected photocurrent measurements were employed. According to the literature,[59] the corrected photocurrent is defined as the device current under illumination as a function of voltage after subtraction of the corresponding dark current ($J_{ph} = J_{light} - J_{dark}$). If the effective applied voltage (V_0–V, where V_0 is the voltage at which the currents measured under illumination and in the dark are equal) is large enough, all carriers generated by light absorption in the active layer will be swept out, leading to a saturated current (J_{sat}). The ratio of J_{ph} to J_{sat} represents the product of the charge separation, transportation and extraction efficiencies. **Figure 6** shows J_{ph}/J_{sat} for PTB7-Th: $PC_{71}BM$ (Binary), PTB7-Th: $PC_{71}BM$: IDIC (S-Ternary) and PTB7-Th: $PC_{71}BM$/IDIC (C-Ternary) based devices over a range of bias (V_0–V). Compared with the Binary device, the S-Ternary device exhibits a lower charge separation efficiency and transportation efficiency, which is the reason for the lower J_{ph}/J_{sat} at low electric field. The J_{ph}/J_{sat} of C-Ternary device at low electric field is higher than that of the Binary device, which is attributed to the enhanced charge extraction efficiency. The J_{ph}/J_{sat} of the C-Ternary device at low electric field is much higher than that of the S-Ternary film due to the enhanced charge separation, transportation and extraction efficiencies.

Figure 6

In summary, we report the concept and design of the donor/acceptor/acceptor ternary OPV with a more controlled structure via sequential solution process. There might be two working mechanisms co-existing in the C-Ternary OPV. The first one is the parallel junction, where two p-n junctions (PTB7-Th/$PC_{71}BM$ and PTB7-Th/IDIC) are formed and work in parallel in active layer. The second one is the p-n junction (PTB7-Th/$PC_{71}BM$) with an n-type layer (IDIC). In this mechanism, the n-type layer near the cathode can improve the electron extraction and block holes to cathode. As a result, compared with simple ternary blend OPV, the C-Ternary OPV exhibits enhanced charge separation, transportation and extraction efficiencies. The PCEs of all four OPV with C-Ternary are enhanced by 14–21% relative to those with simple ternary blend. The best PCEs are 10.7% and 11.0% for fullerene-based (PTB7-Th: $PC_{71}BM$/IDIC) and fullerene-free (PBDB-T: ITIC/IDIC) solar cells, respectively. In addition, a certified PCE of 10.32% (fullerene-free solar cell) is obtained from Newport Corporation. The certified PCE is similar to the average value (10.4%) obtained from our laboratory. Our results demonstrate that the C-Ternary is a potential alternative to the simple ternary blend used in OPV with much higher efficiency.

Experimental Section

Unless stated otherwise, solvents and chemicals were obtained commercially and used without further purification. PTB7-Th[49] was purchased from One-Materials Inc. PBDB-T,[50] ITIC[51] and $PC_{71}BM$ were purchased from Solarmer Inc. IDIC was synthesized according to our previously

reported procedures.[52] 1,8-diiodooctane (DIO), chloroform (CF) and o-dichlorobenzene (DCB) were obtained from Sigma-Aldrich Inc. Organic solar cells were fabricated with the following structure: indium tin oxide (ITO)/zinc oxide (ZnO)/active layer/molybdenum trioxide (MoO_3)/silver (Ag). The ITO glass was pre-cleaned in an ultrasonic bath of acetone and isopropanol, and treated in ultraviolet-ozone chamber (Jelight Company, USA) for 15 min. A thin layer (30 nm) of ZnO sol-gel was spin-coated onto the ITO glass and baked at 200 °C for 60 min. A mixture of PTB7-Th/$PC_{71}BM$ (with 0%, 10%, 15% or 20% IDIC, w/w in the total weight of donor and acceptor) was dissolved in DCB/CF/DIO (100:10:1.5, v/v/v) or DCB/DIO (100:1.5, v/v) mix solvent (D:A=1:2, 18 mg mL^{-1} in total) with stirring overnight (80 °C). A mixture of PTB7-Th/ITIC (with 0% or 15% IDIC, w/w in the total weight of donor and acceptor) was dissolved in DCB/CF (100:10, v/v) mix or DCB solvent (D:A=1:1.5, 15 mg mL^{-1} in total) with stirring overnight (80 °C). A mixture of PBDB-T/$PC_{71}BM$ (with 0% or 15% IDIC, w/w in the total weight of donor and acceptor) was dissolved in DCB/CF/DIO (100:10:3, v/v/v) or DCB/DIO (100:3, v/v) (D:A=1:1, 20 mg mL^{-1} in total) with stirring for 2 h (60 °C). A mixture of PBDB-T/ITIC (with 0% or 15% IDIC, w/w in the total weight of donor and acceptor) was dissolved in DCB/CF/DIO (100:10:0.5, v/v/v) or DCB/DIO (100:0.5, v/v) (1:1, 20 mg mL^{-1} in total) with stirring for 2 h (60 °C). Then, these blend solutions (with CF) were spin-coated on the ZnO layer to form binary or S-Ternary photosensitive layers. For the C-Ternary device, IDIC was dissolved in CF solvent (3, 6 or 9 mg mL^{-1}) with stirring for 1 h (80 °C) and was spin-coated on ZnO layer. After thermal annealing at 80 °C for 10 minutes, the blend solutions (without CF) were spin-coated on the IDIC/ZnO layer to form the C-Ternary photosensitive layers. The thickness of active layer was ca. 100-115 nm. A MoO_3 (ca. 10 nm) and Ag layer (ca. 100 nm) was then evaporated onto the surface of the photosensitive layer under vacuum (ca. 10^{-5} Pa) to form the back electrode. The active area of the device was 0.1

cm^2. The certified cells have the area of 0.0631 cm^2, which is defined by a metal mask with an aperture aligned with the device area.

J–V characteristics of photovoltaic cells were taken using a Keithley 2400 source measure unit under a simulated AM 1.5G spectrum, with an Oriel 9600 solar simulator. EQEs were measured using an integrated system (Enlitech, Taiwan) and a lock-in amplifier with a current preamplifier under short-circuits' condition. Thin-film (on quartz substrate) absorption spectra were recorded on a 4100 Hitachi spectrofluorophotometer. A Horiba Jobin Yvon system with a red light source with an excitation at 660 nm was used to conduct PL measurements. Hole-only or electron-only diodes were fabricated using the following architectures: ITO/poly(3,4-ethylenedioxythiophene): poly(styrenesulfonate) (PEDOT: PSS)/active layer/gold (Au) for holes and aluminium (Al)/active layer/Al for electrons. Mobilities were extracted by fitting the current density-voltage curves using the Mott-Gurney relationship (space charge limited current). Grazing incident wide angle X-ray scattering (GIWAXS) measurement was performed at Advanced Light Source on the 7.3.3. beamline. All the samples were deposited on the silicon wafer with 100 nm silicon oxide. Samples were irradiated by 10 KeV at a fixed X-ray incident angle of 0.14° with an exposure time of 3 s. The samples for X-ray photoelectron spectroscopy (XPS) analysis were spin-coated on ITO glass substrates pre-coated with PEDOT: PSS layer. During the lift-off process in water, the sample films were detached from the ITO glass substrates due to water solubility of PEDOT: PSS layer. As a result, the films of active layer were lifted off and floated on the water. The films were then cut into several pieces (ca. 3 mm × 3 mm). The small pieces of films were transferred to pure Si substrates with selected bottom surface on top. Since both of PTB7-Th, $PC_{71}BM$ and IDIC are insoluble in water, the PTB7-Th molar content does not change after immersing the active layer in water. XPS

measurements were carried out on an XPS AXIS Ultra DLD (Kratos Analytical). An Al Kα (1486.6 eV) X-ray was used as the excitation source. The O/F atom ratios were calculated by the integration of areas of corresponding XPS peaks and the atomic sensitivity factors. The simplified equation is O/F atom ratio = (O Peak area/O sensitivity factor)/(F Peak area/F sensitivity factor).

Supporting Information

Supporting Information is available from the Wiley Online Library or from the author.

Acknowledgements

Y.Y. acknowledged the Air Force Office of Scientific Research (AFOSR) (FA2386-15-1-4108), Office of Naval Research (ONR) (N00014-14-1-0648), National Science Foundation (NSF) (ECCS-1509955), UC-Solar Program (MRPI 328368) for financial support. Part of this research was performed in beamline 7.3.3 in Advanced Light Source Lawrence Berkeley National Laboratory. X.Z. acknowledged the National Science Foundation China (NSFC) (91433114, 21734001) for financial support. All authors acknowledged Ms. Selbi Nuryyeva for English language polish.

Received: ((will be filled in by the editorial staff))
Revised: ((will be filled in by the editorial staff))
Published online: ((will be filled in by the editorial staff))

[1] G. Li, R. Zhu, Y. Yang, *Nat. Photon.* **2012**, *6*, 153.

[2] M. Graetzel, R. A. J. Janssen, D. B. Mitzi, E. H. Sargent, *Nature* **2012**, *488*, 304.

[3] C. J. Brabec, M. Heeney, I. McCulloch, J. Nelson, *Chem. Soc. Rev.* **2011**, *40*, 1185.

[4] Y. F. Li, *Acc. Chem. Res.* **2012**, *45*, 723.

[5] Y. Huang, E. J. Kramer, A. J. Heeger, G. C. Bazan, *Chem. Rev.* **2014**, *114*, 7006.

[6] R. A. J. Janssen, J. Nelson, *Adv. Mater.* **2013**, *25*, 1847.

[7] G. Li, W.-H. Chang, Y. Yang, *Nat. Rev. Mater.* **2017**, *2*, 17043.

[8] P. Cheng, X. Zhan, *Chem. Soc. Rev.* **2016**, *45*, 2544.

[9] J. Zhao, Y. Li, G. Yang, K. Jiang, H. Lin, H. Ade, W. Ma, H. Yan, *Nat. Energy* **2016**, *1*, 15027.

[10] G. A. Chamberlain, *Solar Cells* **1983**, *8*, 47.

[11] C. W. Tang, *Appl. Phys. Lett.* **1986**, *48*, 183.

[12] G. Yu, J. Gao, J. C. Hummelen, F. Wudl, A. J. Heeger, *Science* **1995**, *270*, 1789.

[13] J. J. M. Halls, C. A. Walsh, N. C. Greenham, E. A. Marseglia, R. H. Friend, S. C. Moratti, A. B. Holmes, *Nature* **1995**, *376*, 498.

[14] T. Ameri, P. Khoram, J. Min, C. J. Brabec, *Adv. Mater.* **2013**, *25*, 4245.

[15] L. Lu, M. A. Kelly, W. You, L. Yu, *Nat. Photon.* **2015**, *9*, 491.

[16] P. Cheng, X. Zhan, *Mater. Horiz.* **2015**, *2*, 462.

[17] Q. An, F. Zhang, J. Zhang, W. Tang, Z. Deng, B. Hu, *Energy Environ. Sci.* **2016**, *9*, 281.

[18] L. Yang, L. Yan, W. You, *J. Phys. Chem. Lett.* **2013**, *4*, 1802.

[19] N. Gasparini, X. Jiao, T. Heumueller, D. Baran, G. J. Matt, S. Fladischer, E. Spiecker, H. Ade, C. J. Brabec, T. Ameri, *Nat. Energy* **2016**, *1*, 16118.

[20] L. Yang, H. Zhou, S. C. Price, W. You, *J. Am. Chem. Soc.* **2012**, *134*, 5432.

[21] P. P. Khlyabich, B. Burkhart, B. C. Thompson, *J. Am. Chem. Soc.* **2012**, *134*, 9074.

[22] L. Lu, T. Xu, W. Chen, E. S. Landry, L. Yu, *Nat. Photon.* **2014**, *8*, 716.

[23] J. Zhang, Y. Zhang, J. Fang, K. Lu, Z. Wang, W. Ma, Z. Wei, *J. Am. Chem. Soc.* **2015**, *137*, 8176.

[24] Y. Yang, W. Chen, L. Dou, W.-H. Chang, H.-S. Duan, B. Bob, G. Li, Y. Yang, *Nat. Photon.* **2015**, *9*, 190.

[25] L. Zhong, L. Gao, H. Bin, Q. Hu, Z.-G. Zhang, F. Liu, T. P. Russell, Z. Zhang, Y. Li, *Adv. Energy Mater.* **2017**, *7*, 1602215.

[26] P. P. Khlyabich, B. Burkhart, B. C. Thompson, *J. Am. Chem. Soc.* **2011**, *133*, 14534.

[27] P. Cheng, C. Yan, Y. Wu, J. Wang, M. Qin, Q. An, J. Cao, L. Huo, F. Zhang, L. Ding, Y. Sun, W. Ma, X. Zhan, *Adv. Mater.* **2016**, *28*, 8021.

[28] D. Baran, R. S. Ashraf, D. A. Hanifi, M. Abdelsamie, N. Gasparini, J. A. Rohr, S. Holliday, A. Wadsworth, S. Lockett, M. Neophytou, C. J. M. Emmott, J. Nelson, C. J. Brabec, A. Amassian, A. Salleo, T. Kirchartz, J. R. Durrant, I. McCulloch, *Nat. Mater.* **2017**, *16*, 363.

[29] W. Zhao, S. Li, S. Zhang, X. Liu, J. Hou, *Adv. Mater.* **2017**, *29*, 1604059.

[30] D. H. Wang, D. Y. Kim, K. W. Choi, J. H. Seo, S. H. Im, J. H. Park, O. O. Park, A. J. Heeger, *Angew. Chem. Int. Ed.* **2011**, *50*, 5519.

[31] V. Janković, Y. Yang, J. You, L. Dou, Y. Liu, P. Cheung, J. P. Chang, Y. Yang, *ACS Nano* **2013**, *7*, 3815.

[32] J. M. Lee, B.-H. Kwon, H. I. Park, H. Kim, M. G. Kim, J. S. Park, E. S. Kim, S. Yoo, D. Y. Jeon, S. O. Kim, *Adv. Mater.* **2013**, *25*, 2011.

[33] H. J. Kim, J.-H. Kim, J.-H. Ryu, Y. Kim, H. Kang, W. B. Lee, T.-S. Kim, B. J. Kim, *ACS Nano* **2014**, *8*, 10461.

[34] B. Fan, C. Sun, X.-F. Jiang, G. Zhang, Z. Chen, L. Ying, F. Huang, Y. Cao, *Adv. Funct. Mater.* **2016**, *26*, 6479.

[35] Y. Zhang, H. Zhou, J. Seifter, L. Ying, A. Mikhailovsky, A. J. Heeger, G. C. Bazan, T.-Q. Nguyen, *Adv. Mater.* **2013**, *25*, 7038.

[36] N. D. Treat, J. A. Nekuda Malik, O. Reid, L. Yu, C. G. Shuttle, G. Rumbles, C. J. Hawker, M. L. Chabinyc, P. Smith, N. Stingelin, *Nat. Mater.* **2013**, *12*, 628.

[37] P. Cheng, C. Yan, T.-K. Lau, J. Mai, X. Lu, X. Zhan, *Adv. Mater.* **2016**, *28*, 5822.

[38] P. Cheng, M. Zhang, T.-K. Lau, Y. Wu, B. Jia, J. Wang, C. Yan, M. Qin, X. Lu, X. Zhan, *Adv. Mater.* **2017**, *29*, 1605216.

[39] B. M. Savoie, S. Dunaisky, T. J. Marks, M. A. Ratner, *Adv. Energy Mater.* **2015**, *5*, 1400891.

[40] P. P. Khlyabich, A. E. Rudenko, R. A. Street, B. C. Thompson, *ACS Appl. Mater. Interfaces* **2014**, *6*, 9913.

[41] N. Li, F. Machui, D. Waller, M. Koppe, C. J. Brabec, *Sol. Energy Mater. Sol. Cells* **2011**, *95*, 3465.

[42] A. L. Ayzner, C. J. Tassone, S. H. Tolbert, B. J. Schwartz, *J. Phys. Chem. C* **2009**, *113*, 20050.

[43] D. Chen, F. Liu, C. Wang, A. Nakahara, T. P. Russell, *Nano Lett.* **2011**, *11*, 2071.

[44] B. Yang, Y. Yuan, J. Huang, *J. Phys. Chem. C* **2014**, *118*, 5196.

[45] D.-H. Kim, J. Mei, A. L. Ayzner, K. Schmidt, G. Giri, A. L. Appleton, M. F. Toney, Z. Bao, *Energy Environ. Sci.* **2014**, *7*, 1103.

[46] J. J. van Franeker, S. Kouijzer, X. Lou, M. Turbiez, M. M. Wienk, R. A. J. Janssen, *Adv. Energy Mater.* **2015**, *5*, 1500464.

[47] Y. Wang, X. Zhan, *Adv. Energy Mater.* **2016**, *6*, 1600414.

[48] M. Ghasemi, L. Ye, Q. Zhang, L. Yan, J.-H. Kim, O. Awartani, W. You, A. Gadisa, H. Ade, *Adv. Mater.* **2017**, *29*, 1604603.

[49] S.-H. Liao, H.-J. Jhuo, Y.-S. Cheng, S.-A. Chen, *Adv. Mater.* **2013**, *25*, 4766.

[50] D. Qian, L. Ye, M. Zhang, Y. Liang, L. Li, Y. Huang, X. Guo, S. Zhang, Z. a. Tan, J. Hou, *Macromolecules* **2012**, *45*, 9611.

[51] Y. Lin, J. Wang, Z.-G. Zhang, H. Bai, Y. Li, D. Zhu, X. Zhan, *Adv. Mater.* **2015**, *27*, 1170.

[52] Y. Lin, Q. He, F. Zhao, L. Huo, J. Mai, X. Lu, C.-J. Su, T. Li, J. Wang, J. Zhu, Y. Sun, C. Wang, X. Zhan, *J. Am. Chem. Soc.* **2016**, *138*, 2973.

[53] G. G. Malliaras, J. R. Salem, P. J. Brock, C. Scott, *Phys. Rev. B* **1998**, *58*, 13411.

[54] M. Campoy-Quiles, T. Ferenczi, T. Agostinelli, P. G. Etchegoin, Y. Kim, T. D. Anthopoulos, P. N. Stavrinou, D. D. C. Bradley, J. Nelson, *Nat. Mater.* **2008**, *7*, 158.

[55] Z. Xu, L. M. Chen, G. W. Yang, C. H. Huang, J. H. Hou, Y. Wu, G. Li, C. S. Hsu, Y. Yang, *Adv. Funct. Mater.* **2009**, *19*, 1227.

[56] X. Guo, N. Zhou, S. J. Lou, J. Smith, D. B. Tice, J. W. Hennek, R. P. Ortiz, J. T. L. Navarrete, S. Li, J. Strzalka, L. X. Chen, R. P. H. Chang, A. Facchetti, T. J. Marks, *Nat. Photon.* **2013**, *7*, 825.

[57] Z. Xiao, Y. Yuan, B. Yang, J. VanDerslice, J. Chen, O. Dyck, G. Duscher, J. Huang, *Adv. Mater.* **2014**, *26*, 3068.

[58] J. Huang, J. H. Carpenter, C.-Z. Li, J.-S. Yu, H. Ade, A. K. Y. Jen, *Adv. Mater.* **2016**, *28*, 967.

[59] M. A. Faist, S. Shoaee, S. Tuladhar, G. F. A. Dibb, S. Foster, W. Gong, T. Kirchartz, D. D. C. Bradley, J. R. Durrant, J. Nelson, *Adv. Energy Mater.* **2013**, *3*, 744.

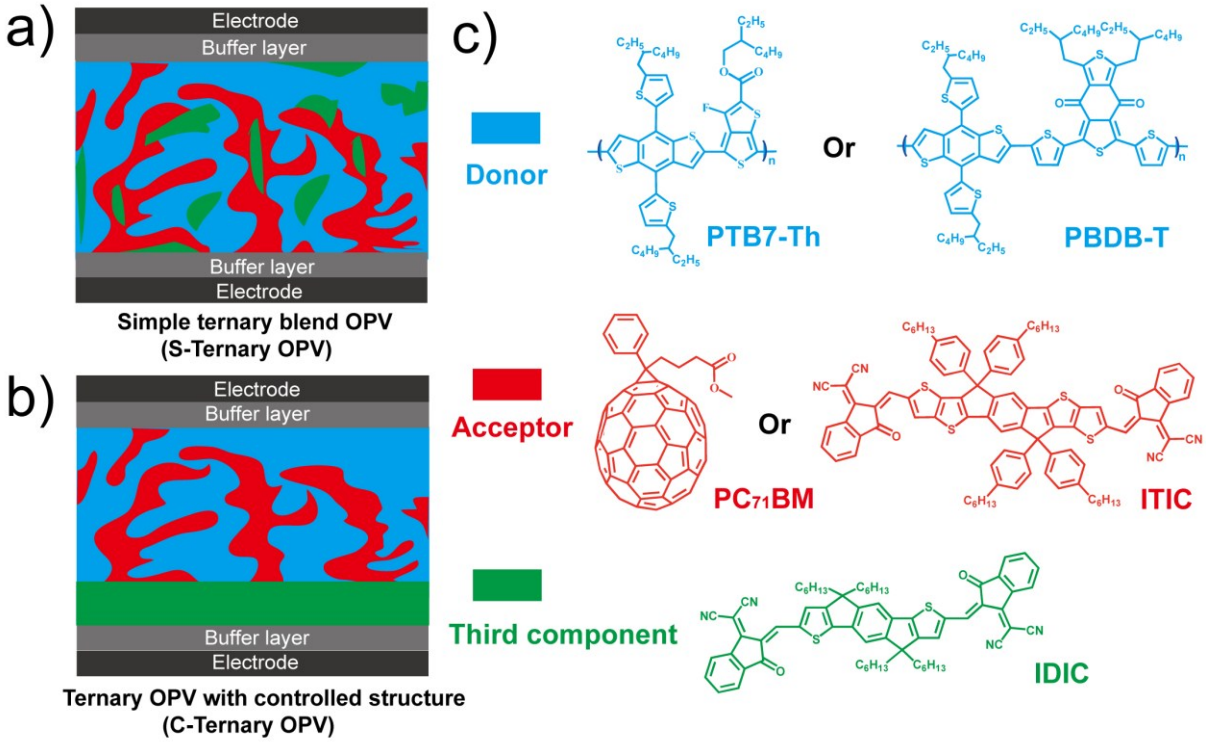

Figure 1. a) Schematic diagrams of S-Ternary OPV and b) C-Ternary OPV. c) Molecule structures of donors (PTB7-Th, PBDB-T), acceptors ($PC_{71}BM$, ITIC) and the third component (IDIC).

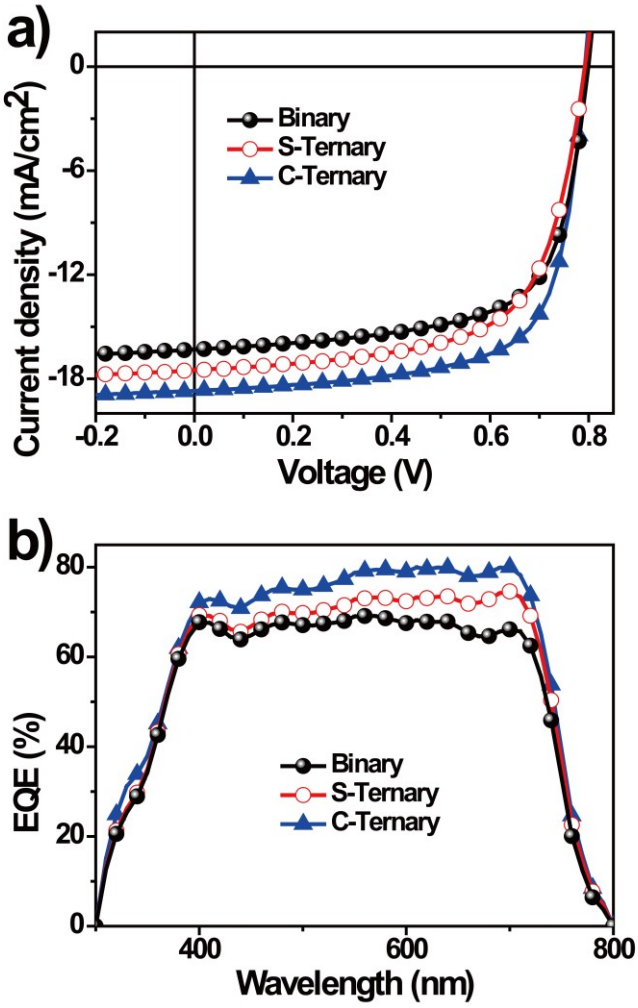

Figure 2. a) *J–V* curves and b) EQE spectra of devices based on PTB7-Th: $PC_{71}BM$ (Binary), PTB7-Th: $PC_{71}BM$: IDIC (S-Ternary) and PTB7-Th: $PC_{71}BM$/IDIC (C-Ternary) under the illumination of an AM 1.5G solar simulator, 100 mW cm^{-2}.

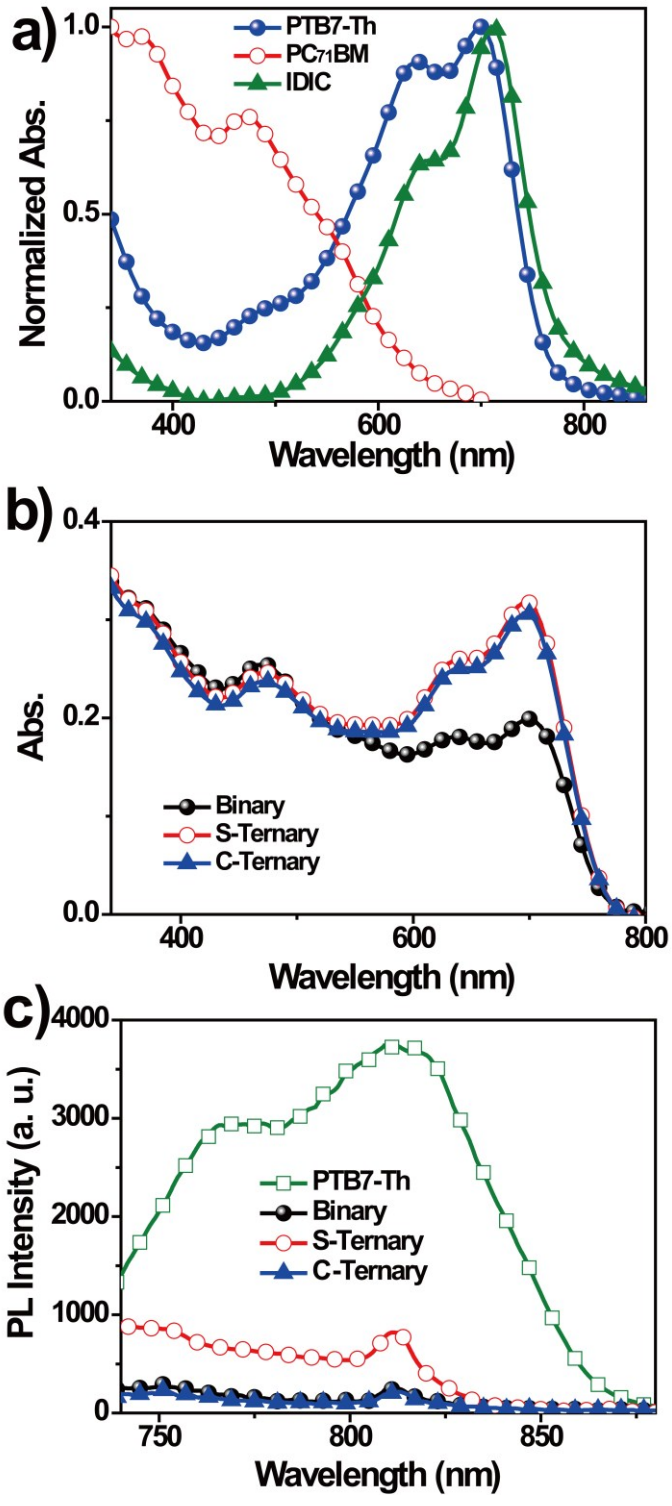

Figure 3. a) Absorption spectra of pure PTB7-Th, $PC_{71}BM$ and IDIC films. b) Absorption spectra and c) PL spectra of PTB7-Th: $PC_{71}BM$ (Binary), PTB7-Th: $PC_{71}BM$: IDIC (S-Ternary) and PTB7-Th: $PC_{71}BM$/IDIC (C-Ternary) films.

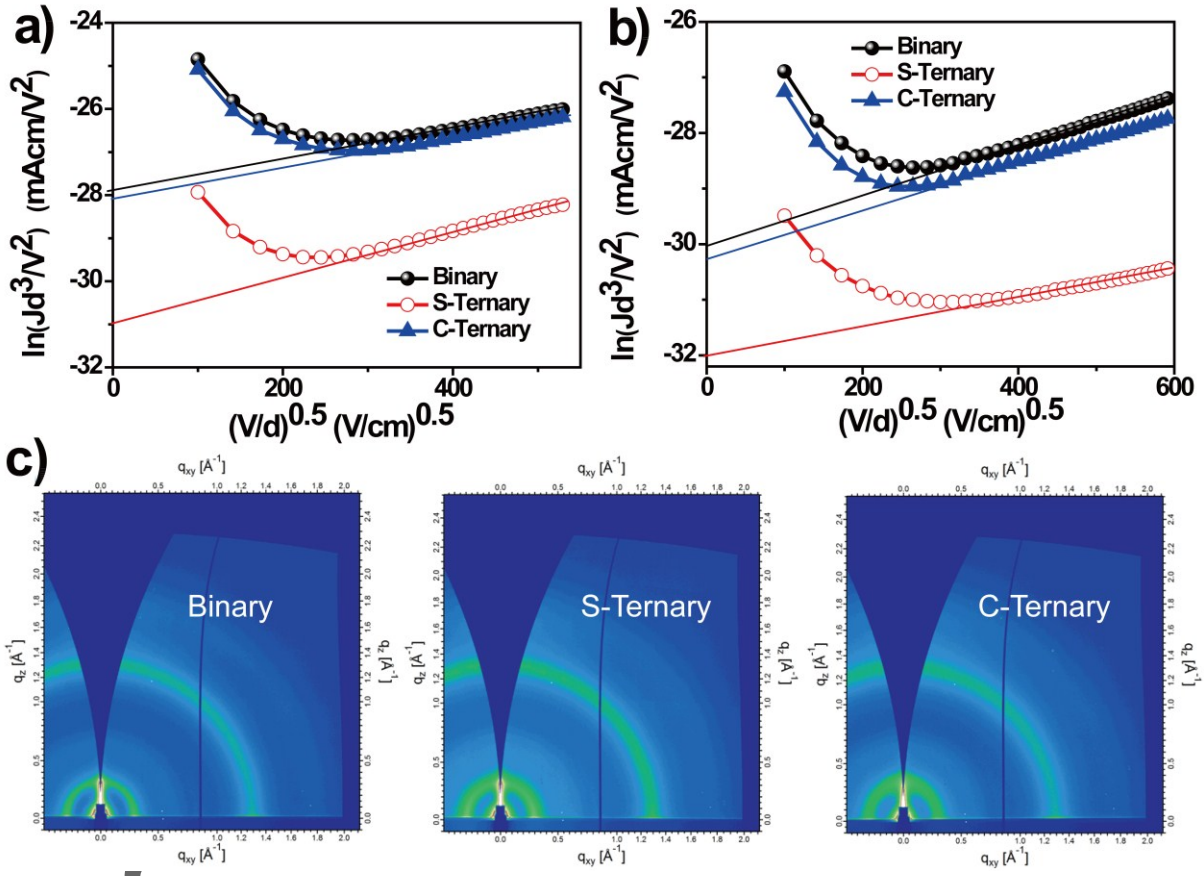

Figure 4. a) Measured *J–V* characteristics under dark for hole-only devices, b) Measured *J–V* characteristics under dark for electron-only devices and c) 2D GIWAXS patterns based on PTB7-Th: $PC_{71}BM$ (Binary), PTB7-Th: $PC_{71}BM$: IDIC (S-Ternary) and PTB7-Th: $PC_{71}BM$/IDIC (C-Ternary) films.

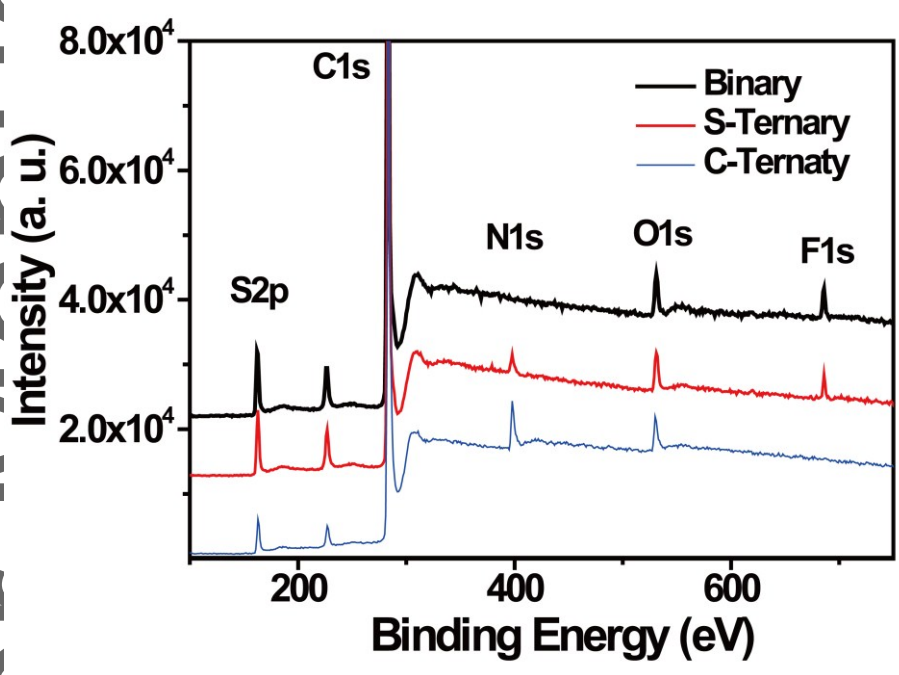

Figure 5. XPS survey scans of PTB7-Th: $PC_{71}BM$ (Binary), PTB7-Th: $PC_{71}BM$: IDIC (S-Ternary) and PTB7-Th: $PC_{71}BM$/IDIC (C-Ternary) films on bottom surface.

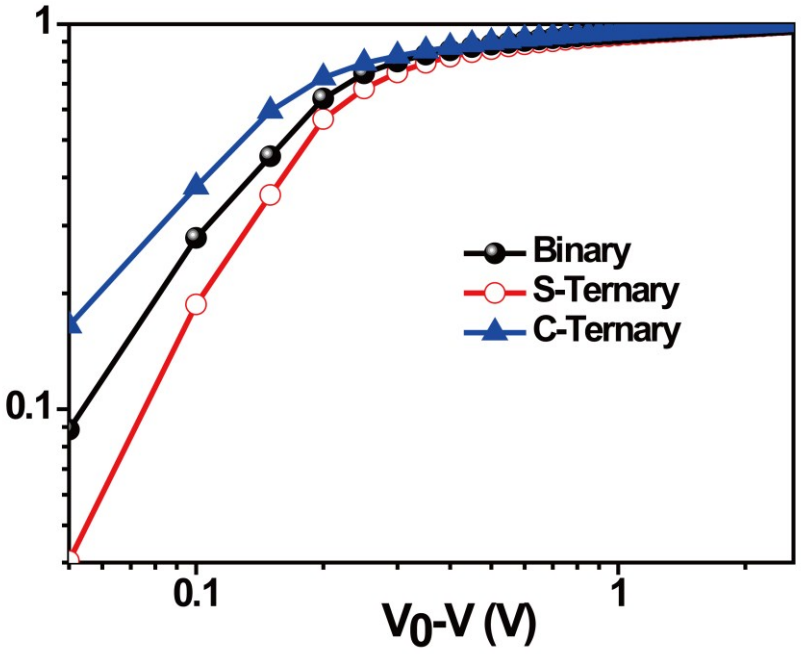

Figure 6. Corrected photocurrent data as a function of the potential difference V_0–V. Data are presented for the devices based on PTB7-Th: $PC_{71}BM$ (Binary), PTB7-Th: $PC_{71}BM$: IDIC (S-Ternary) and PTB7-Th: $PC_{71}BM$/IDIC (C-Ternary) films.

Table 1. Average and the best device data based on PTB7-Th: $PC_{71}BM$ or PTB7-Th: ITIC without or with IDIC as the third component (S-Ternary or C-Ternary).

Active layer	Structure	V_{OC} (V)	J_{SC} (mA cm^{-2})	Calculated J_{SC} (mA cm^{-2})	FF (%)	PCE (%)	
						average	best
PTB7-Th: $PC_{71}BM$ (1:2)	Binary	0.80±0.01	16.3±0.3	15.8	67.2±0.4	8.8±0.2	9.1
PTB7-Th: $PC_{71}BM$: IDIC (1:2:0.45)	S-Ternary	0.79±0.01	17.5±0.4	16.9	64.9±0.5	9.0±0.2	9.3
PTB7-Th: $PC_{71}BM$ (1:2)/IDIC (15 nm)	C-Ternary	0.79±0.01	18.7±0.4	18.2	69.6±0.6	10.3±0.3	10.7
PTB7-Th: ITIC (1:1.5)	Binary	0.80±0.01	15.3±0.4	15.1	62.1±0.3	7.6±0.3	8.0
PTB7-Th: ITIC: IDIC (1:1.5:0.375)	S-Ternary	0.80±0.01	16.3±0.4	15.8	60.0±0.4	7.8±0.3	8.2
PTB7-Th: ITIC (1:1.5)/IDIC (15 nm)	C-Ternary	0.80±0.01	17.6±0.5	17.1	64.2±0.3	9.0±0.3	9.5
PTB7-Th: IDIC (1:1)	Binary	0.80±0.01	11.5±0.3	11.2	55.3±0.4	5.1±0.2	5.4

Table 2. Average and the best device data based on PBDB-T: $PC_{71}BM$ or PBDB-T: ITIC without or with IDIC as the third component (S-Ternary or C-Ternary).

Active layer	Structure	V_{OC} (V)	J_{SC} (mA cm^{-2})	Calculated J_{SC} (mA cm^{-2})	FF (%)	PCE (%)	
						average	best
PBDB-T: $PC_{71}BM$ (1:1)	Binary	0.88±0.01	11.6±0.3	11.3	66.0±0.2	6.7±0.2	7.0
PBDB-T: $PC_{71}BM$: IDIC (1:1:0.3)	S-Ternary	0.88±0.01	12.7±0.2	12.5	62.4±0.4	7.0±0.2	7.3
PBDB-T: $PC_{71}BM$ (1:1)/IDIC (15 nm)	C-Ternary	0.88±0.01	14.3±0.5	14.0	67.5±0.3	8.5±0.4	9.0
PBDB-T: ITIC (1:1)	Binary	0.90±0.01	14.3±0.4	14.1	68.1±0.5	8.8±0.3	9.2
PBDB-T: ITIC: IDIC (1:1:0.3)	S-Ternary	0.90±0.01	14.8±0.3	14.6	66.6±0.3	8.9±0.3	9.4
PBDB-T: ITIC (1:1)/IDIC (15 nm)	C-Ternary	0.90±0.01	16.0±0.4	15.8	72.3±0.5	10.4±0.4	11.0
PBDB-T: IDIC (1:1)	Binary	0.89±0.01	12.1±0.4	11.7	63.1±0.3	6.8±0.3	7.2

Table 3. Hole mobilities and electron mobilities of PTB7-Th: $PC_{71}BM$ without or with IDIC as the third component (S-Ternary or C-Ternary).

Active layer	Structure	μ_h ($cm^2 V^{-1} s^{-1}$)	μ_e ($cm^2 V^{-1} s^{-1}$)
PTB7-Th: $PC_{71}BM$ (1:2)	Binary	4.1×10^{-3}	5.5×10^{-4}
PTB7-Th: $PC_{71}BM$: IDIC (1:2:0.45)	S-Ternary	2.0×10^{-4}	7.5×10^{-5}
PTB7-Th: $PC_{71}BM$ (1:2)/IDIC (15 nm)	C-Ternary	3.7×10^{-3}	4.1×10^{-4}

The table of contents entry

The concept and design of ternary organic photovoltaics with a more controlled structure via sequential solution process was reported. The power conversion efficiencies of all four organic photovoltaics (fullerene-based or fullerene-free) with this structure were enhanced by 14–21% relative to those with simple ternary blend.

Keyword: solar cell

Pei Cheng, Rui Wang, Jingshuai Zhu, Wenchao Huang, Sheng-Yung Chang, Lei Meng, Pengyu Sun, Hao-Wen Cheng, Meng Qin, Chenhui Zhu, Xiaowei Zhan and Yang Yang*

Ternary System with Controlled Structure: A New Strategy towards Efficient Organic Photovoltaics